Japanese Journal of Applied Physics
Vol. 47, No. 10, 2008, pp. 0000–0000

Self-Assembled Growth and Characterization of Mn_xP Nanowires

Katsuaki SATO[1,2], Alexei BOURAVLEUV[1,3], Akinori KOUKITU[1], and Takayuki ISHIBASHI[4]

[1]*Graduate School of Engineering, Tokyo University of Agriculture and Technology, Nakacho, Koganei, Tokyo 184-8588, Japan*
[2]*Office of Basic Research, Japan Science and Technology Agency, Sambancho, Chiyoda-ku, Tokyo 102-0075, Japan*
[3]*A.F. Ioffe Physico-Technical Institute, 194021 St. Petersburg, Russian Federation*
[4]*Department of Materials Science and Technology, Nagaoka University of Technology, Kamitomioka, Nagaoka, Niigata 940-2188, Japan*

(Received December 28, 2007; accepted July 31, 2008; published online xxxx yy, zzzz)

MnP nanowires have been grown by molecular beam epitaxy (MBE) without any preliminary deposited metal catalyst on InP(100) and $GaAs(111)_B$ substrates. Mn was supplied using a conventional Knudsen cell, whereas P_2 was supplied as a gas by the decomposition of tertiary butylphosphine (TBP) using a cracking cell. The self-assembled growth of nanowires was observed when the substrate temperature exceeded 430 °C. Nanowires obtained on the InP(100) surface had diameters close to 150 nm, lengths of up to 2 μm, whereas nanowires grown on the $GaAs(111)_B$ surface had widths of up to 600 nm, lengths of up to 30 μm, and clear atomic facets. Magnetic and optical characterizations were also carried out.
[DOI: 10.1143/JJAP.47.dummy]

KEYWORDS: nanowire, manganese phosphide, magnetic properties, ellipsometry

1. Introduction

The fabrication of nanowires is attracting attention due to their versatility for device applications.[1,2)] Compared with the growth of nanowires using the conventional vapor–liquid–solid (VLS) mechanism, which requires the use of metal-catalyst nanoparticles,[2–4)] catalyst-free (or self-catalytic) methods[5–8)] have advantages for the creation of new devices, because they avoid contamination of nanowires from a metal catalyst as well as to obtain completely self-assembled formation of nanowires.

The present work is devoted to an investigation of the self-catalytic growth of Mn_xP nanowires and their properties. Bulk orthorhombic MnP is a very promising material because it exhibits very interesting physical properties such as ferromagnetism with a relatively high Curie temperature ($T_c = 291.5$ K),[9)] a first-order transition from ferromagenetic to screw magnetism at 47 K,[10)] and a large magnetocaloric effect.[11)] Therefore, the creation of Mn_xP-based one-dimensional nanostructures might have even more potential for spintronics applications, which has not yet been thoroughly investigated.

Recently a method of synthesizing of MnP nanorods by the solution-phase thermal decomposition of continuously delivered Mn-tri-*n*-octylphosphine (TOP) complex using a syringe pump was reported.[12)] According to the report, uniformly sized MnP nanorods of 8 nm in width and 16–22 nm in length were obtained. Magnetic measurements revealed that the MnP nanorods had a T_c of around 292 K with a relatively high blocking temperature (T_B) of 260 K.

In this paper we report on the characterization of Mn_xP nanowires grown by molecular beam epitaxy (MBE).

2. Experiments

Mn_xP nanowires were first discovered to grow simultaneously with Ge nanowires during the MBE growth of $MnGeP_2$ thin films.[13)] In this study MnP and Mn_2P nanowires were grown by MBE without any preliminary deposited metal catalyst on InP(100) and $GaAs(111)_B$ substrates. Mn vapor was supplied from a solid source using a conventional Knudsen cell, whereas P_2 was supplied by the decomposition of tertiary butylphosphine (TBP) using a cracking cell. The growth time was varied from 30 min to 2 h. The temperature of the substrates was held at 480–545 °C. The growth of nanowires was not observed for temperatures below 435 °C. The flow rate of TBP was set in the range of 2.0–2.3 sccm using a mass flow controller. The TBP was cracked at about 830 °C to ensure that the P_2 component remained dominant. The temperature of the Mn Knudsen cell was varied in the range of 630–660 °C.

The nanowires were characterized using a scanning electron microscope (SEM) and a scanning transmission electron microscope (STEM) with an energy-dispersive X-ray spectrometer (EDX), as well as an X-ray diffraction (XRD) system. The STEM measurements were carried out at the Art, Science and Technology Center, Kyushu University. The magnetic properties were measured at Institute for Materials Research (IMR), Tohoku University using a superconducting quantum interference device (SQUID) in the temperature range of 2–350 K. Optical data were obtained using a JASCO M-220 spectroscopic ellipsometer at wavelengths of 260–860 nm at room temperature.

3. Results and Discussion

3.1 *Crystallographic properties and growth mechanism*

Typical microstructures of the self-assembled nanowires obtained on InP(100) and $GaAs(111)_B$ surfaces are shown in Figs. 1 and 2, respectively. The SEM images demonstrate that the nanowires grown on InP and GaAs substrates differ not only in size but also in crystallographic shape. Nanowires obtained on the InP(100) surface have average diameters of 50–150 nm and lengths of up to 2 μm depending on the temperature and gas supply rate. The size distribution in each growth experiment was comparatively uniform with a standard deviation of less than 10%. On the other hand, nanowires grown on the $GaAs(111)_B$ surface have well-defined atomic facets with widths of 100–600 nm and lengths of up to 30 μm (see Fig. 2) with a less uniform size distribution than those on the InP(100) surface as shown in Fig. 1.

As mentioned above, in our growth procedure we did not deposit any preliminary metal catalyst layer such as gold. Nonetheless, it was found that some of the nanowires grown at higher temperatures on InP substrates have a more complicated structure consisting of two parts, similar to the nanowires obtained by the VLS growth mechanism using

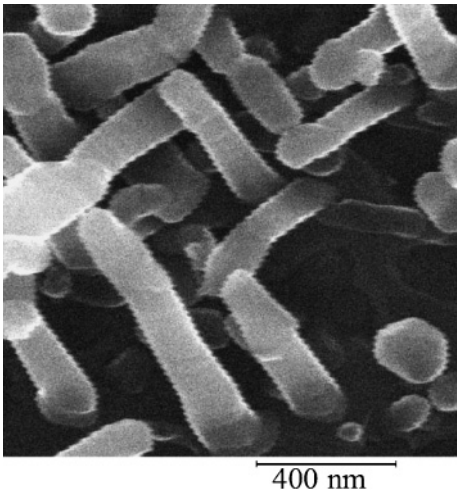

Fig. 1. SEM image of nanowires grown on InP(100) substrate (T_{growth} = 510 °C).

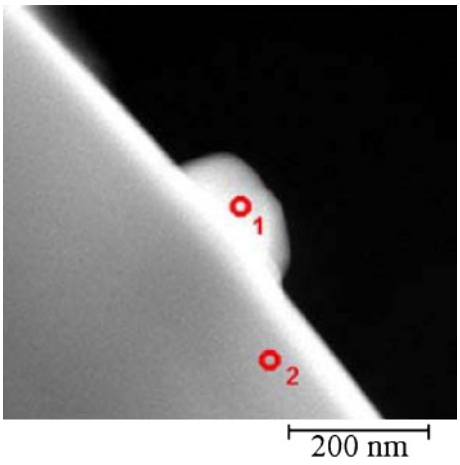

Fig. 3. (Color online) STEM image of Mn-based nanocluster on InP(100) substrate. Point 1—composition of Mn : P ~ 20 : 14%, point 2—composition = InP 100%.

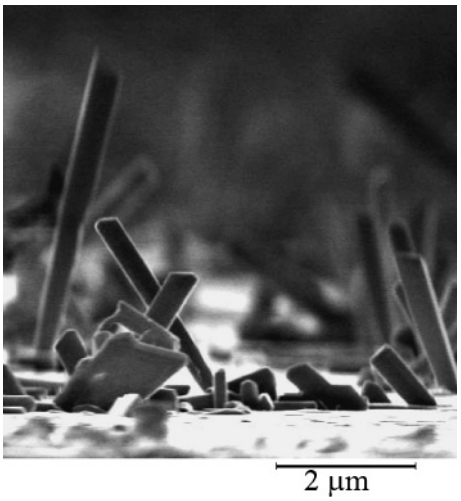

Fig. 2. SEM image of nanowires grown on GaAs(111)$_B$ substrate (T_{growth} = 535 °C).

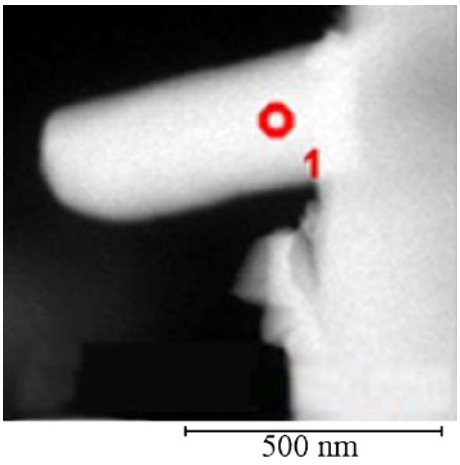

Fig. 4. (Color online) STEM image of nanowire grown on GaAs(111)$_B$ substrate. Point 1—composition of Mn : P ~ 48.8 : 25.4% (~Mn_2P).

metal catalyst nanoclusters as seeds for the growth. The density of such nanowires increased with the growth time. Moreover, STEM investigations revealed that the growth of nanowires on both GaAs(111)$_B$ and InP(100) surfaces is apt to be caused by the formation of Mn-based nanoclusters on the substrate surface (see Fig. 3). It seems likely that the crystallographic structure of Mn-based nanoclusters and the shapes of nanowires depend on the reconstructed surface structure of the substrates. However, the process of nucleation of the Mn-based nanoclusters has not yet been thoroughly investigated, although it is a goal of one of our current studies.

The study of the chemical composition of elements in nanowires was performed by EDX analyses. The results obtained showed that the chemical composition of the nanowires grown on the GaAs(111)$_B$ substrate is close to the Mn_2P phase (see Fig. 4). On the top of the nanowires no precipitated droplets of other phases were found.

Such self-catalytic growth of nanowires appears to be partially explained by considering a diffusion-induced mechanism.[8] According to this mechanism, due to their low chemical potential the top surface of nanowires attracts adatoms that diffuse on the side facets towards the tip. The shapes of nanowires can vary depending on the relation between the diffusion length and the size of the nanowires. If the length of a nanowire l is longer than the diffusion length λ, the nanowire tends to be tapered toward the tip end. In the case of the GaAs substrate under our growth conditions, no nanowires of this type were observed, suggesting that l is less than λ in this case, whereas for the growth on the InP(100) surface such nanowires were observed.

Further evidence for the diffusion-induced mechanism was found during the STEM–EDX observation of the nanowires. Some of the nanowires obtained (see Fig. 5) surprisingly contained a part (for example, point 1 in Fig. 5) that can be related to the InP phase despite the fact that our MBE apparatus is not equipped with an indium supply source. It should be noted, however, that most of the nanowires grown on the InP substrate had a chemical composition corresponding to the MnP phase (see Fig. 6). Since the density of such nanowires was found to depend on the growth temperature and the growth time, it is supposed that MnP nanowires that nucleated at an initial stage of the growth act as a catalyst for the growth of InP nanowires. The source of the In atoms diffusing on the side facets may be

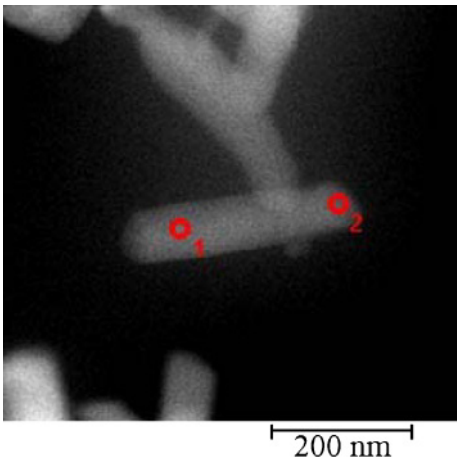

Fig. 5. (Color online) STEM image of nanowire grown on InP(100) substrate. Point 1—composition of In : Mn : P ~ 34.47 : 13.2 : 36.5%. Point 2—composition of In : Mn : P ~ 6.04 : 40.87 : 42.24%.

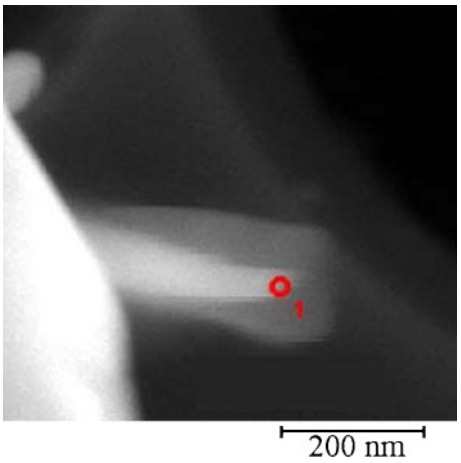

Fig. 6. (Color online) STEM image of nanowire grown on InP(100) substrate. Point 1—composition of Mn : P ~ 38.50 : 38.48% (= MnP).

those evaporated from the InP substrate, with the rate of evaporation increasing at elevated temperatures, and with increasing growth time. In this way, a new potential method for the growth of nanowires using atoms evaporated from the host substrate as building materials can be considered.

3.2 *Magnetic properties*

The magnetic properties of the samples were studied using a VSM magnetometer in the temperature range of 77–300 K. It was found that the samples obtained on $GaAs(111)_B$ substrates did not exhibit any ferromagnetic ordering in this temperature range, which is consistent with the data on the chemical composition (Mn : P = 2 : 1) of the nanowires obtained by EDX, since it is known that bulk Mn_2P is antiferromagnetic. In contrast, the samples with nanowires grown on the InP(100) substrates showed ferromagnetic behavior at room temperature.[14)]

The temperature dependences of the magnetization measured with an applied field of 100 Oe for the MnP nanowires on InP after zero-field cooling (curve 1) and field cooling (curve 2) are shown in Fig. 7(a). The overall features of the magnetization–temperature (M–T) curve are similar to those of bulk MnP. The Curie temperature T_c of the samples was

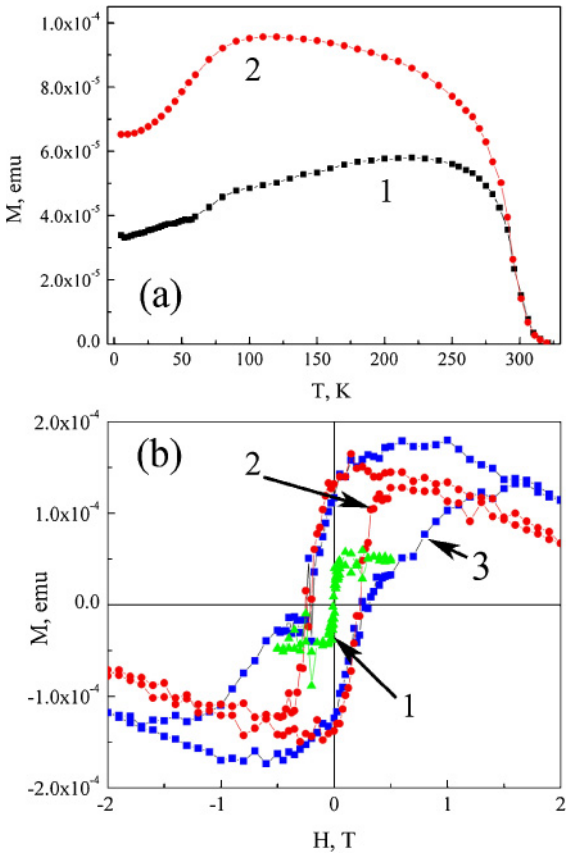

Fig. 7. (Color online) (a) Temperature dependences of magnetization measured with an applied field of 100 Oe for the sample with MnP nanowires after zero-field cooling (curve 1) and field cooling (curve 2). (b) Magnetic-field dependences of magnetization measured at 295 K (curve 1), 220 K (curve 2), and 15 K (curve 3).

found to be ~291 K, which is close to the value obtained for bulk MnP. In addition, a drop in the magnetization below 100 K is observed in curve 2, reflecting the complicated magnetic phase diagram for the bulk material.[15)] The divergence of the nonfield-cooling and field-cooling curves is observed around 270 K; this temperature is close to the reported blocking temperature (260 K). The results of the measurements of the field dependences of the magnetization (M–H) curve shown in Fig. 7(b) demonstrate the presence of clearly resolved hysteresis loops up to 280 K. The value of the coercive field (H_c), which persists up to 220 K, was 3000 Oe. Moreover, at low temperatures [see curve 3 in Fig. 7(b)] a double-hysteresis-like loop was observed, suggesting that the sample is magnetically inhomogeneous. The reason for the existence of the higher coercive field, which is equal to 7000 Oe at low temperatures, is still unclear but can be associated with the existence of a ferromagnetic semiconductor phase of Mn-doped InP.[16,17)]

3.3 *Optical properties*

In Fig. 8 are shown spectra of the imaginary part of the dielectric function, i.e., ε'', which correspond to the absorption spectra of the samples. Curve 1 corresponds to the sample covered with nanowires grown on the InP(100) substrate prepared at the substrate temperature of 510 °C. For comparison, the ε'' spectra for the InP substrate and for the polished surface of a bulk MnP single crystal are shown

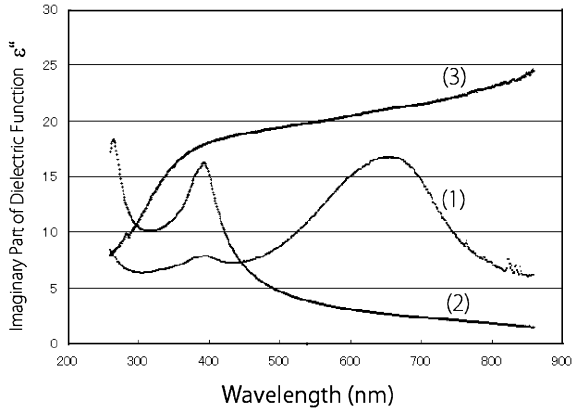

Fig. 8. Spectra of the imaginary part of the dielectric function obtained by spectroscopic ellipsometry for the sample with MnP nanowires grown on the InP(100) substrate (curve 1), the InP(100) substrate surface (curve 2), and the polished surface of a MnP single crystal (curve 3).

as curves 2 and 3, respectively. The ε'' spectrum of the sample with nanowires (curve 1) has a main peak around 650 nm. In addition to the main peak, small peaks around 265–395 nm are observed, which may reasonably be attributed to the optical effect from the portions of the InP surface not covered with nanowires, since these wavelengths agree with those in the ε'' spectrum of InP shown as curve 2. We therefore assign the main peak around 650 nm ($\sim$1.9 eV) to an optical transition in the nanowires. However, no corresponding structure is found in the MnP bulk spectrum shown by curve 3. The featureless broad absorption band increasing toward a longer wavelength in curve 3 can be associated with optical transitions from the majority-spin 3d band situated at 0.7–2.7 eV below the Fermi level (E_F) to empty 3p band states above E_F, taking into account the calculated spin-polarized energy band structure of MnP.[18] Therefore, the observed 650 nm absorption peak in the nanowire cannot be assigned to the above-mentioned band-to-band transition and its origin should be elucidated through future investigations.

4. Conclusions

The self-assembled growth of nanowires of binary compounds consisting of Mn and P on InP(100) and GaAs(111)$_B$ substrates has been performed by MBE without any metal catalyst nanoclusters. Nanowires grown on the GaAs(111)$_B$ substrate possess the chemical composition of the Mn_2P phase, which is antiferromagnetic, whereas those on the InP substrate are of the MnP phase, which is ferromagnetic at room temperature. Some of the nanowires grown on InP are inhomogeneous and the partial existence of an InP:Mn phase is suggested, which appears to cause an additional coercive field to MnP hysteresis. The growth mechanism of this self-catalytic growth is discussed in terms of the diffusion-induced mechanism, instead of the conventional VLS mechanism.

The optical properties of nanowires were investigated by spectroscopic ellipsometry, and were compared with those of an InP substrate and a MnP single crystal.

Acknowledgments

This work was conducted under the 21st Century COE Program “Future Nano Materials” of Tokyo University of Agriculture and Technology. Dr. A. Bouravleuv thanks Japan Society for Promotion of Science (JSPS) for the financial support (Grant P 06112). This work was partly supported by the Nanotechnology Support Project of the Ministry of Education, Culture, Sports, Science and Technology, Japan (Project No. 16-556). We thank Professor S. Mitani of Tohoku University for his help in SQUID measurements, and Professor N. Kuwano and Dr. H. Sosiati of Kyushu University for STEM–EDX observations. We also thank Professor K. Yamada of Tohoku University for supplying a MnP single crystal.

1) W. Lu and C. M. Lieber: J. Phys. D **39** (2006) R387.
2) H. J. Fan, P. Werner, and M. Zacharias: Small **2** (2006) 700.
3) R. S. Wagner: *Whisker Technology* (Wiley, New York, 1970).
4) K. Hiruma, M. Yazawa, T. Katsuyama, K. Ogawa, K. Haraguchi, and M. Koguchi: J. Appl. Phys. **77** (1995) 447.
5) C. J. Novotny and P. K. L. Yu: Appl. Phys. Lett. **87** (2005) 203111.
6) M. Mattila, T. Hakkarainen, and H. Lipsanen: Appl. Phys. Lett. **89** (2006) 063119.
7) B. W. I. Park, G. C. Yi, M. Kim, and S. J. Pennycook: Adv. Mater. **14** (2002) 1841.
8) R. K. Debnath, R. Meijers, T. Richter, T. Stoica, R. Calarco, and H. Luth: Appl. Phys. Lett. **90** (2007) 123117.
9) E. E. Huber, Jr. and D. Ridgley: Phys. Rev. **135** (1964) A1033.
10) T. Komatsubara, H. Shinohara, T. Suzuki, and E. Hirahara: J. Appl. Phys. **40** (1969) 1037.
11) M. S. Reis, R. M. Rubinger, N. A. Sobolev, M. A. Valente, K. Yamada, K. Sato, Y. Todate, A. Bouravleuv, P. J. von Ranke, and S. Gama: Phys. Rev. B **77** (2008) 104439.
12) J. Park, B. Koo, K. Y. Yoon, Y. Hwang, M. Kang, J. G. Park, and T. Hyeon: J. Am. Chem. Soc. **127** (2005) 8433.
13) A. D. Bouravleuv, K. Minami, T. Ishibashi, and K. Sato: Phys. Status Soldi A **203** (2006) 2793.
14) A. D. Bouravleuv, S. Mitani, R. M. Rubinger, M. C. Carmo, N. A. Sobolev, T. Ishibashi, A. Koukitu, and K. Sato: Physica E **40** (2008) 2037.
15) A. Zieba, C. C. Becerra, H. Fjellvag, N. F. Oliveira, and A. Kjekshus: Phys. Rev. B **46** (1992) 3380.
16) P. Poddar, Y. Sahoo, H. Srikanth, and P. N. Prasad: Appl. Phys. Lett. **87** (2005) 062506.
17) T. M. Schmidt, P. Venezuela, J. T. Arantes, and A. Fazzio: Phys. Rev. B **73** (2006) 235330.
18) A. Yanase and A. Hasagawa: J. Phys. C **13** (1980) 1989.